J Solid State Electrochem (2018) 22:1483–1493
https://doi.org/10.1007/s10008-017-3805-y

ORIGINAL PAPER

Electrochemical and associated techniques for the study of the inclusion complexes of thymol and β-cyclodextrin and its interaction with DNA

Katherine Lozano[1] · Fabricia da Rocha Ferreira[1] · Emanuella G. da Silva[1] · Renata Costa dos Santos[1] · Marilia O. F. Goulart[1] · Samuel T. Souza[2] · Eduardo J. S. Fonseca[2] · Claudia Yañez[3] · Paulina Sierra-Rosales[4] · Fabiane Caxico de Abreu[1]

Received: 15 July 2017 / Revised: 3 September 2017 / Accepted: 10 October 2017 / Published online: 29 October 2017

Abstract Thymol, a potent agent for microbial, fungal, and bacterial disease, has low aqueous solubility and it is genotoxic, i.e., is capable of damaging deoxyribonucleic acid (DNA). This possible problem of DNA toxicity needs to be solved to allow the use of different doses of thymol. This study characterized the inclusion compound containing thymol and β-cyclodextrin (β-CD) by measuring the interaction between these two components and the ability of thymol to bind DNA in its free and β-CD complexed form. The encapsulation approach using β-CD is particularly useful when controlled target release is desired, and a compound is insoluble, unstable, or genotoxic. The interaction between thymol and DNA has been studied using electrochemical quartz crystal microbalance (EQCM), atomic force microscopy (AFM), and differential pulse voltammetry (DPV). The characterization of the inclusion complex of thymol and β-CD was analyzed by UV-vis spectrophotometry, cyclic voltammetry, and scanning electrochemical microscopy (SECM). Based on the free β-CD by spectrophotometry method, the association constant of thymol with the β-CD was estimated to be 2.8×10^4 L mol^{-1}. The AFM images revealed that in the presence of small concentrations of thymol, the dsDNA molecules appeared less knotted and bent on the mica surface, showing significant damage to DNA. The SECM and voltammetry results both demonstrated that the interaction of thymol-β-CD complex was smaller than the free compound showing that the encapsulation process may be an advantage leading to a reduction of toxic effects and increase of the bioavailability of the drug.

Keywords Thymol · β-Cyclodextrin · AFM · SECM · EQCM · DPV

✉ Fabiane Caxico de Abreu
caxico.fabiane@gmail.com

[1] Instituto de Química e Biotecnologia, Universidade Federal de Alagoas, Maceió, AL 57072-900, Brazil

[2] Grupo de Óptica e Nanoscopia (GON), Instituto de Física, Universidade Federal de Alagoas, Maceió, AL 57072-900, Brazil

[3] Centro de Investigación de los Procesos Redox (CiPRex), Facultad de Ciencias Químicas y Farmacéuticas, Universidad de Chile, 8380492 Santiago, Chile

[4] Programa Institucional de Fomento a la Investigación, Desarrollo e Innovación, Universidad Tecnológica Metropolitana, Ignacio Valdivieso 2409, P.O. Box 8940577, Santiago, San Joaquín, Chile

Introduction

Thymol is a natural phenol found in various plant species, including the Lamiaceae and Verbenaceae families [1]. Thymol (2 isopropyl-5 methyl phenol, Scheme 1) is a major component of the essential oils extracted from *Thymus vulgaris* (40% oil) and *Lippia sidoides* (66% oil) [2–4]. For centuries, thymol has been used to flavor home remedies, perfume, and insecticide. Medicinally, it is used as a spasmolytic, antibacterial, antifungal, expectorant, antiseptic, anthelmintic, and antitussive [4–6]. These properties are attributed to the presence of phenolic compounds such as thymol, carvacrol, and hydrocarbons [7–9]. Thymol alone is toxic to larvae of *B. microplus* [10] and a potent antioxidant [2, 3], therefore exhibiting larvicidal and repellent properties.

Thyme volatiles, principally thymol and the other phenol compounds, and carvacrol are usually present in human food, beverages, pharmaceuticals, perfumes, and cosmetics [11, 12]. Thymol is present at low levels in human food; however, if the

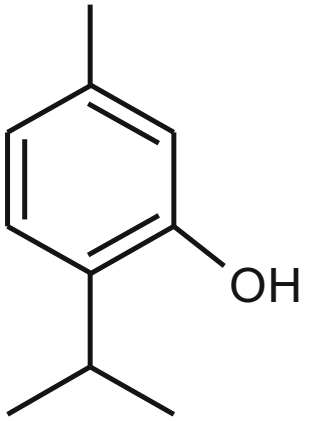

Scheme 1 Thymol chemical structure of thymol

use of this compound is extended to other applications that may require higher doses, the increased exposure of humans to thymol is a matter of concern.

There are no studies available on the genotoxicity of thymol testing acute and short-term effects in vivo, and a few reports are available about the damage to DNA in the presence of thymol [14–17]. Therefore, it is not easy to predict real exposure tolerances for consumers. The genotoxicity potential at a low degree of thymol is suggested to be weak in SOS-Chromotest and DNA repair test, both performed in *Escherichia coli* [13]. High levels of genotoxicity are reported with substantial DNA damage using sister chromatid exchange and comet tests in bone marrow and lung fibroblast mouse, respectively [14, 15].

Other relevant studies have been investigated in human peripheral lymphocytes. For instance, Aydin and coworkers [16] evaluated thymol genotoxicity in human lymphocytes by use of the single-cell gel electrophoresis assay, reporting no increase in DNA strand breakage for non-toxic doses of thymol (concentrations below 0.1 mmol L^{-1}). However, it was observed that higher concentration of 0.2 mmol L^{-1} the damage to DNA increased. On the other hand, Buyukleyla [17] reported that thymol induced an increase of sister chromatid exchange (SCE) and structural chromosome aberration (CA), particularly in the lower concentrations in human peripheral lymphocytes.

The use of β-cyclodextrin (β-CD) to encapsulate hydrophobics substances has garnered increased interest over the past decade given its potential role in improving drug delivery regimens. Cyclodextrins (CDs) are cyclic oligosaccharides, consisting of D-glucopyranose units (α-1,4)-linked with a somewhat lipophilic central cavity and a hydrophilic outer surface and are known to, among many other skills, decrease the toxicity of substances included in its cavity [18–20]. Encapsulations in CDs have been used extensively to increase the solubility, stability, bioavailability, protection against oxidation, and delivery of the active components in food, pharmaceutical, and cosmetic industries, in addition to decrease genotoxicity [19–21]. Thymol exhibits several of these characteristic properties and represents a potential candidate for complexation with CD as a promising delivery and possible inclusion complex to decrease a possible thymol toxicity. Therefore, special attention must be taken in its use and in the development of methodologies like encapsulation in β-CD to minimize toxicity effects for high doses of thymol [15, 17].

Mulinacci and coworkers [22] studied the conformational structure of the thymol-β-CD complex using H1 NMR and molecular modeling techniques. They found that two possible complexes could be formed since both structures have the same conformational energy values. The experimental data, however, revealed the complex that exists in real solution is that one having the hydrogens of the isopropyl group of thymol on the side of the hydrophobic cavity of β-CD [22]. Additionally, microencapsulation of thymol with β-CD was described by Tao and coworkers [23]. They described the successful synthesis and characterization of that complex used for natural antimicrobial delivery for food safety. Taking into account that efficient formation of inclusion complexes with cyclodextrins is achieved, it may be used to decrease the genotoxicity and increase the solubility of the thymol.

To the best of our knowledge, there are no studies investigating encapsulation of thymol using β-CD, their electrochemical properties, and their genotoxic activity together. In the present work, we reported the characterization of the inclusion complex of thymol and β-CD by measuring the interaction between these two components and the ability of thymol to bind DNA in its free and complexed form. This work is divided in two sections. The first section determinates the DNA-binding properties of thymol that are reflective of genotoxicity by differential pulse voltammetry (DPV), electrochemical quartz crystal microbalance (EQCM), and atomic force microscopy (AFM). In the second section, we investigated the DNA-binding properties of thymol and cyclodextrin-thymol inclusion complexes by cyclic voltammetry, UV-vis spectrophotometry, and scanning electrochemical microscopy (SECM).

Experimental

Materials

β-Cyclodextrin (β-CD) and calf thymus double-stranded DNA (dsDNA, length about 1000 bp) were purchased from Sigma-Aldrich (USA) and used without further purification. Thymol was obtained from ECIBRA. The stock thymol solution (c = 1.0 mmol L^{-1}) was prepared by dissolving the compound in ethanol. Ferrocene carboxylic acid (Fc-CO_2H) and sodium methoxide (($NaOCH_3$) were obtained from Alfa

Aesar. 11-Mercaptoundecanoic acid (MUA) was obtained from Merck.

The dsDNA was used for the AFM experiments. The dsDNA solution was prepared by dissolving 0.5 μg/mL ctDNA in buffer containing 10 mmol L^{-1} HEPES, pH 7, and 1 mmol L^{-1} $NiCl_2$. In the same way, thymol was diluted to 0.5 g/L in a buffer containing 10 mmol L^{-1} HEPES, pH 7. HEPES was obtained from Applied Biosystems (USA). All reagents used were of the highest purity. All the buffer solutions were prepared using analytical grade reagents and water purified in a Millipore Milli-Q system (conductivity < 0.1 μS cm^{-1}).

Spectrophotometric measurements

A UV-vis spectrophotometer (Shimadzu) was used to measure and analyze the inclusion of thymol in the cavity of free β-CD. An aqueous solution of thymol (1.0×10^{-4} mol L^{-1}) was prepared with 1.5% (*v*/*v*) ethanol. Seven aliquots of 25 mL of this solution were removed and mixed with appropriate amounts of β-CD to obtain concentrations of 5.0×10^{-5}–7.0×10^{-4} mol L^{-1} of β-CD. The mixtures were stirred (170 rpm) for 1 h at 25 °C. Absorbance values were measured in the wavelength range of 240–368 nm. The constant of formation was determined based on the average value of the absorbance measured.

Electrochemical studies

Cyclic voltammetry (CV) and differential pulse voltammetry (DPV) experiments were performed using an Autolab PGSTAT-30 potentiostat from Echo Chemie (Utrecht, Netherlands) coupled to a PC microcomputer with GPES 4.9 software with a conventional three-electrode cell. The working electrode was a glassy carbon (GC) (d = 3 mm) from Bioanalytical System (BAS); the counter electrode was a Pt wire, and the reference was a Cl^- saturated (Ag/AgCl), all contained in a one-compartment electrochemical cell, with a volumetric capacity of 10 mL. The GC electrode was polished with 0.3 and 0.05 μm alumina on a polishing pad (BAS polishing kit) and washed with water. After mechanical cleaning, electrochemical pre-treatment of the GC electrode involved a sequence of 10 cyclic potential scans from −1.2 to +1.4 V in 0.1 mol L^{-1} H_2SO_4 solution. Argon was used to avoid contact with oxygen at the solution during the experiments.

The electrochemical studies of thymol were conducted in a protic medium using cyclic and pulse differential voltammetry techniques in glassy carbon and a SAM-modified gold electrode and the scan rate (0.020–1.0 Vs^{-1}) and pH effects were investigated.

Preparation of SAM-modified gold electrode

The monolayer preparation of SAM electrode of HS-β-CD was built upon the gold bead electrode by immersing it for 20 h in a solution containing an appropriate ratio of HS-β-CD, MUA, and ferrocene carboxyl acid in the mixed solvent (DMSO: EtOH: H_2O = 5:3:2, *v*/*v*/*v*) [24]. The modified electrode was denoted as CD-SAM electrode. This electrode was prepared by dropping this solution (5 μL, three times) onto the gold electrode (GE) and then heating it at less than 60 °C to remove the solvent [25].

After optimizing experimental parameters for the proposed CD-SAM electrode, the analytical curve was built up by the addition of aliquots of stock thymol solution into a measurement cell containing phosphate buffer solution 0.2 M, pH 7.

Electrochemical quartz crystal microbalance

The dsDNA was immobilized on self-assembled monolayers on gold electrodes for electrochemical quartz crystal microbalance. The bare electrode (Au-quartz crystal, Methron, 6 MHz) was first immersed in a 40 μmol L^{-1} aminothiol solution for 6 h to obtain a SAM-modified gold electrode (SAM/Au). The SAM/Au electrode was placed in contact with 1 mg mL^{-1} dsDNA in the presence of 1 mg mL^{-1} 1-ethyl-3-(3-dimethyl aminopropyl) carbodiimide hydrochloride (EDAC) in a 40 mmol L^{-1} 2-[N-morpholino]ethanesulfonic acid (MES) buffer (pH 5.6) for 1 h, applying a potential at 0.0 V [26]. A SAM-modified GE with dsDNA was obtained and was denoted as dsDNA/SAM/GE.

AFM images experiments

The mica surface was prepared for imaging by treatment with poly-L-lysine. A drop of 0.02% solution of poly-L-lysine was applied to the surface of freshly cleaved mica. Then, it was then incubated for 15 min and gently rinsed with 2 mL of deionized water. Finally, the mica was gently blown dry with argon gas to minimize surface contamination. dsDNA (5 ng DNA, diluted in 10 mmol L^{-1} HEPES and 1 mmol L^{-1} $NiCl_2$) was then pipetted on mica treated for 10 min, rinsed, and allowed to dry completely under a flow of clean argon gas. It was stored in a vacuum cabinet under argon for an hour to allow optimum sample drying; 5.0×10^{-2} mmol L^{-1} thymol was added to the mica fixed with DNA and incubated for 10 min, rinsed with 3 mL of deionized water and dried under a continuous flow of argon gas. Finally, it was stored in a vacuum cabinet for 1 h.

The AFM images were taken in the air with a Multiview 1000TM AFM (Nanonics, Israel) operating in Tapping Mode, mounted on a dual light Olympus microscope (BXFM). AppNano (California, USA) silicon cantilevers ACT-SS with nominal spring constants between 36 and 75 N/m were used.

The typical tapping frequency was 270–300 KHz, the nominal scanning rate was typically 1.5 Hz per line, and the modulation amplitude was a few nanometers [27–29]. All images presented in this report derive from the original data except that the images were processed by flattening to remove the background slope. Also, the complete setup was acoustically isolated to reduce the interference of ambient noise during the measurements.

Differential pulse voltammetry of ssDNA in the presence of the thymol

Single-stranded DNA (ssDNA) was produced by acid-base treatment of dsDNA. The dsDNA (1 mg) was dissolved in 1.0 mol L^{-1} HCl (100 μL) by heating (at 100 °C) in a sealed glass tube in a boiling water bath for 1 h, followed by neutralization with 1.0 M NaOH [30]. The solution was completed using acetate buffer. This solution was added to the electrochemical cell and single-scan DPV experiments were conducted in the range 0 to +1.4 V vs. Ag|AgCl, Cl^- (0.1 mol L^{-1}), using the following DPV parameters: pulse amplitude of 50 mV, step potential of 10 mV, scan rate of 10 mVs^{-1}, and modulation time of 50 ms. The GCE was immersed into a solution containing thymol, β-CD, and thymol:β-CD inclusion complex (with different β-CD concentrations: from 0.1 to 10 mmol L^{-1}) and ssDNA, and the DPV experiment was repeated. A clean GCE was also employed in DPV experiments with a 0.05 mmol L^{-1} solution of thymol alone, and the current of the peak was used for comparison purposes. All results of thymol ssDNA experiments were compared to the blank (1 mL of EtOH/acetate buffer solution (20%), pH 4.5, without thymol).

Scanning electrochemical microscopy

Scanning electrochemical microscopy (SECM) was performed with a CHI 900 setup (CH Instruments Inc., USA). A homemade carbon fiber with 10-μm-diameter ultramicroelectrode (UME) was employed as the SECM tip while a GCE with a 3 mm diameter (Model CHI104, CH Instruments) was used as the SECM substrate. The auxiliary and reference electrodes were a Pt wire and Ag/AgCl/KCl(sat) electrode, respectively. The modified electrode was made after immobilization of dsDNA on the surface (12 mg/mL acetate buffer).

SECM experiments were performed using the feedback mode. The experiments were carried out in 0.2 mol L^{-1} phosphate buffer, PBS, pH 7.4, using ferrocene methanol (FcOH) as the redox mediator. The tip potential was held at 0.500 V to produce the oxidation of FcOH, while the potential of the bare or modified GCE (called the substrate) was kept at 0.000 V to allow for feedback between the electrodes (for more details about the SECM procedure see ref. [31]).

Results and discussions

Interaction of thymol with DNA by electrochemical quartz crystal microbalance, atomic force microscopy images, and differential pulse voltammetry

Electrochemical quartz crystal microbalance experiments

Of the various methods and techniques used to study damage to DNA caused by toxic substances and environmental pollutants, EQCM enables observation of the interaction of a substance with the DNA by increasing the mass deposited on the surface of a quartz crystal [32, 33].

Amplification of the oligonucleotide-DNA sensing processes by the electronic transduction of the recognition event by microgravimetric quartz crystal microbalance assay has been reported in the literature [33]. Here we report on the recognition of dsDNA using functionalized gold crystal and an electrochemical quartz crystal microbalance (EQCM) through amplification and electronic transduction, respectively. EQCM measurements are employed to investigate the dsDNA-binding properties of thymol.

Electronic dsDNA sensors were assembled. The aminothiol was assembled on an Au-quartz crystal and acts as the sensing interaction interface between the functionalized transducer and the dsDNA. The amount of composite deposited in the Au-quartz crystal was determined before and after the interaction of dsDNA with 40 μM amine-thiol. Figure 1 shows the EQCM transduction of the amplified sensing of the analyte and the interaction of the functionalized crystal with the thymol. An accumulation of 3.95×10^{15} molecules of thymol by square centimeter on the dsDNA surface was observed, demonstrating the interaction of the compound with the macromolecule. The above results indicated that mass gain has happened on the dsDNA modified Au-quartz crystals.

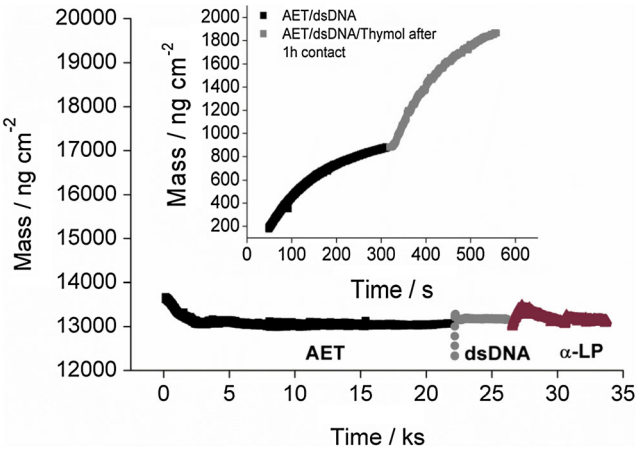

Fig. 1 EQCM of the interaction between dsDNA and thymol. Graph shows a time-dependent mass changes on the crystal. *AET* amine ethanol deposition, *α-LP* α-lapachone. Inset: dsDNA deposition and interaction with dsDNA with thymol

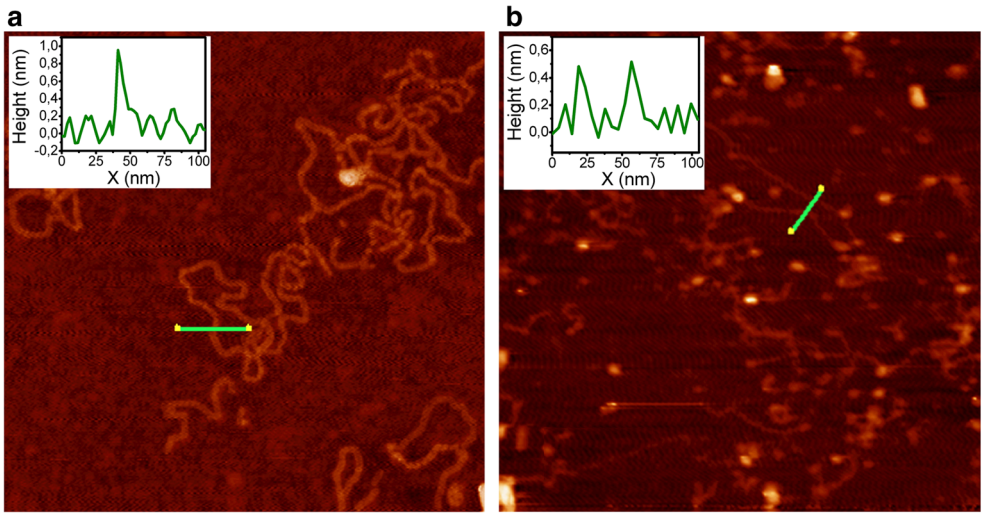

Fig. 2 Atomic force microscopic images of bound DNA in the absence and presence of 0.05 mmol L^{-1} thymol. These DNA samples are prepared using poly-L-lysine onto mica surface. The image (**a**) DNA on mica treated with poly-L-lysine. The image (**b**) DNA on mica treated with poly-L-lysine and thymol. The heights of the DNA strands were 1 and 0.5 nm in the absence and presence of thymol, respectively (upper left image). Both images were obtained by a semi-contact technique in air. Image scan area for each figure corresponds 1 μm × 1 μm

There is one possible reason for the mass gain explained by thymol molecules intercalated into dsDNA.

Atomic force microscopy experiments

Atomic force microscopy (AFM) image of DNA in the air is a convenient alternative to electron microscopy for determining conformations of DNA and DNA-ligand complex [27, 33]. Some researchers have reported that AFM is a reliable option for determining DNA damage for non-toxic doses in different compounds and it is supported by several genotoxicity assays where DNA damage has been demonstrated [34, 35].

Mica is a layered mineral with a negative surface charge, and DNA is a negatively charged polymer. Thus, positive charge probably binds DNA to mica by bridging the negative charges on the DNA and the mica. The modification of mica surface using poly-L-lysine provides a vigorous and firm bond with DNA [36]. This strong fixation of DNA allows the study of DNA conformational change on mica when interacting with thymol. The DNA-thymol complex on the mica shows excellent information of alterations or conformational changes in the DNA strands. The results from imaging DNA/ poly-L-lysine mica samples are shown in Fig. 2. The image illustrates that DNA strands are distributed over the surface (Fig. 2a). In Fig. 2b, the DNA-thymol complex on the mica shows alterations or conformational changes in the DNA strands. These changes were measured with the heights of the DNA strands. Any change in the height of the DNA control shows drastic DNA changes after contact with thymol. As shown in the Fig. 2b, the height of 0.5 nm of DNA-thymol complex shows conformational changes not observed for DNA strands without thymol. The height of 1 nm of DNA strands represents a control image (Fig. 2a).

In this work, we used 0.05 mmol L^{-1} thymol to evaluate its genotoxicity, and we have found relevant information of toxicity with DNA despite the low level of thymol. These findings are supported by two critical studies where the genotoxicity of thymol, using comet assay and sister chromatid exchange was examined. The results from comet test indicated some clastogenic DNA damage in V79 Chinese hamster lung fibroblast cells treated with 0.025 mmol L^{-1} thymol [15]. Also, has been reported DNA damage in rat bone marrow cells for non-toxic doses of thymol [14].

The genotoxicity of thymol in human lymphocytes have been investigated by evaluating the genotoxicity of thymol for several doses (concentrations below 0.1 mmol L^{-1}). Others results indicated strong DNA damage for all concentrations of thymol confirmed by the increase of sister chromatid exchange (SCE) and structural chromosome aberration (CA) in human peripheral lymphocytes [17]. Aydin [16] and Ündeger [15] also reported that thymol induces breaks in DNA strand at concentrations above 50–100 mmol L^{-1}, resulting in the clastogenic effect of DNA.

Taking into account a previous reported study about DNA damage, it has been established that the sites of interaction of thymol with dsDNA occur by hydrogen bonds in the hydroxyl group of phenol, principally the N7 atoms of guanine and the N3 of cytosine [37]. Hydrogen bond also occurs with the O_2 atoms of thymine, the N7 of adenine and, a high concentration of thymol. There is also an interaction with the phosphate skeleton.

It can be concluded that the genotoxic potential of thymol in DNA is high, although it worked with a lower level of thymol. Therefore, the use of encapsulation of thymol with β-cyclodextrin offers a promising application to minimize genotoxicity effects for toxic doses of thymol.

Differential pulse voltammetry of ssDNA in the presence of thymol

The electrochemical behavior of ssDNA in presence of thymol, β-CD, and thymol: β-CD inclusion complex was

evaluated by differential pulse voltammetry (DPV). As shown in Fig. 3, DPV was run in protic medium, acetate buffer pH 4.5 on the glassy carbon electrode (GCE). The ssDNA voltammogram showed two peaks centered at 960 and 1240 mV (Fig. 3).The peaks described below were characterized for purine bases taking into account the characteristic potential of each base.

In the presence of thymol ,three peaks were observed. The first peak at 770 mV corresponds to the oxidation of thymol, and the next two peaks corresponds to the oxidation of the DNA bases. It is clear that the oxidation peak currents of ssDNA are largely decreased (51% for guanosine and 83% for adenosine) and the oxidation peaks potentials are slightly shifted to more positive values. This behavior proves that thymol interacts with guanine and adenine DNA bases. In the same way, the β-CD and the inclusion complex (thymol:β-CD) were also tested. When ssDNA interacts with β-CD, there is a decrease of 24% of the peak current for guanosine and 31% of the peak current of adenosine. This probably is due to hydrogen bond formation between the oligosaccharide and the ssDNA. Thus, confirming a possible interaction between ssDNA and β-CD. When thymol is encapsulated for β-CD, the peak associated to the oxidation of thymol still appears but the intensity of the peak is smaller than the obtained with thymol alone. This indicates that the redox center of thymol is partially introduced into the β-CD cavity. Also, for the purine bases, no shift in peak potentials were observed.

Mulinacci [22] proposed a model that includes molecular modeling and confirmed by ^{1}H NMR and NOE. They showed that the complex formed between thymol and β-CD, the phenolic hydroxyl, its main functional group, is next to the secondary oligosaccharide hydroxyl, then forming hydrogen bonding. This allows us to conclude that when encapsulated, thymol is partially unavailable to interact with the active sites of DNA, which probably reduces its toxicity.

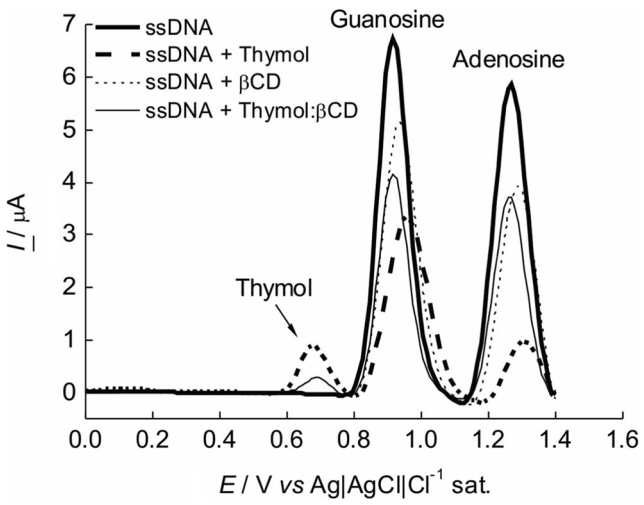

Fig. 3 Difference pulse voltammograms of ssDNA on glassy carbon electrodes in 0.2 mmol L^{-1} acetate buffer solution (pH 4.5) containing 0.05 mmol L^{-1} thymol, β-cyclodextrin, and thymol: β-CD inclusion complex

In this first section, the data obtained by EQCM and AFM showed that thymol, even in non-toxic doses, strongly interacts with DNA to cause breaks the double helix. Also, this damage is confirmed more precisely in adenine and guanine bases by DPV using ssDNA in solution. The study by DPV proves that thymol forms inclusion complex with β-CD and interacts strongly with DNA, respectively. The DPV results have also consisted with the EQCM further confirmed the interaction between DNA and thymol was reasonable. Thus, the encapsulation may represent a strategy to combat or decrease thymol toxicity. So the second section, of the experiments were focused on the electrochemical methods and UV-vis spectrophotometric to study the thymol-*β-CD* complex in addition to the use of the scanning electrochemical microscopy (SECM) to understand the effect of the thymol- *β-CD* complex on DNA and their resulting genotoxicity effects.

Electrochemical, spectrophotometric, and scanning electrochemical microscopy DNA analysis with an inclusion complex of thymol and beta-cyclodextrin (thymol-*β-CD* complex)

The interaction mechanism between thymol-*β-CD* complex and dsDNA was characterized by electrochemical methods, UV-vis spectrophotometric, and SECM.

Electrochemical DNA analysis of thymol-β-CD complex

Structural studies of the inclusion compounds of thymol, and the other phenol compounds in β-CD were quite studied by cyclic voltammetry (CV) [14, 15, 23]. CV was run for 1.0 mmol L^{-1} thymol in absence and presence of several β-CD concentrations on the glassy carbon electrode (GCE) in 0.2 mol L^{-1} Na_2SO_4. An oxidation peak was observed at 612 mV in the absence of β-CD, which means the thymol characteristic potential is centered at this position. To analyze the effect of the thymol encapsulation in β-CD, three different β-CD concentrations were evaluated. As shown in Fig. 4, an initial increase in the peak current was observed up to a molar ratio of [β-CD]/[Thymol] = 0.1due increase of solubility. A further increase of β-CD concentration caused a decrease in the oxidation peak current and a positive shift in the peak potential. A further decrease and anodic shift of potential can be explained by the formation of an inclusion complex with β-CD. Once an electroactive guest forms a stable inclusion complex with a β-CD host, the corresponding electrochemical reaction is suppressed in the complex.

The formation constant complex was determined by electrochemical experiments, using the self-assembled monolayer (SAM) of a β-CD modified electrode (SAM HS-β-CD).

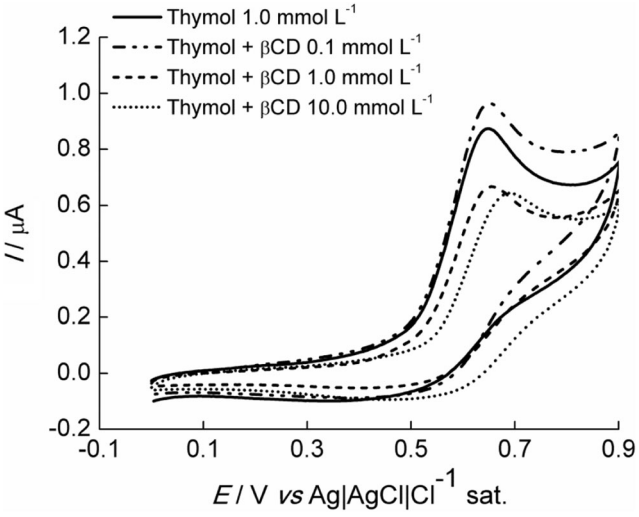

Fig. 4 Cyclic voltammograms for 1.0 mmol L^{-1} thymol on GCE scanned at 100 mVs^{-1} in 0.2 mmol L^{-1} Na_2SO_4 (pH 7.0), in the absence (solid line) and presence of three different β-CD concentrations (broken lines)

Firstly, the formation of the SAM of a β-CD modified electrode was confirmed by the absence of peaks of $Fe(CN)_6^{3-}$ (Fig. 5, curve a) and the presence of redox peaks of $FcCO_2H$ (Fig. 5, curve b), used as an electroactive marker for cyclic voltammetry since it undergoes encapsulation in β-CD. This behavior is expected for $Fe(CN)_6^{3-}$ because of its size, which is larger than the cavity of the β-CD, precludes its arrival on the surface, and hence, its detection. On the other hand, the β-CD monolayer does not suppress Fc-CO_2H redox processes, indicating that it is possible to build selective systems based on this mixed monolayer film SH β-CD and MUA [38, 39]. The HS-β-CD-modified electrode showed an irreversible voltammetry response in the presence of 6×10^{-5} mol L^{-1} thymol suggesting an inclusion process (Fig. 5, curve c).

Also, we have estimated the apparent surface coverage by using the following equation (Eq. (1)):

$$\Gamma = Q_t/nFAe \quad (1)$$

where Q_t is charge from the area under the desorption wave of the thiolate cyclodextrin, and all other symbols have their usual meanings. In the present case, the calculated surface coverage Γ is 3.43×10^{-11} mol cm^{-2}.

The potential dependence of the peak currents on the concentration of thymol in the solution was investigated using cyclic voltammetry technique. As shown in Fig. 6, our results exhibited a peak current saturated at a high concentration of thymol. Also, the graph shows a similar shape to that expected for a Langmuir adsorption isotherm. Thus, the association stability constant of the complex was calculated according to the following equation: [38, 39] (Eq. (2)):

$$\frac{[Thymol]_0}{I} = \frac{1}{KI_{max}} + \frac{[Thymol]_0}{I_{max}} \quad (2)$$

where I is the peak current when the initial concentration of thymol is $[Thymol]_0$, I_{max} is the maximum peak current, and K is the association inclusion constant of thymol with surface-confined β-CD. The K value was calculated to be 3.46×10^4 L mol^{-1}.

Spectrophotometric measurements

A UV-vis spectrophotometric investigation of the interaction between thymol and β-CD was performed. To determine the

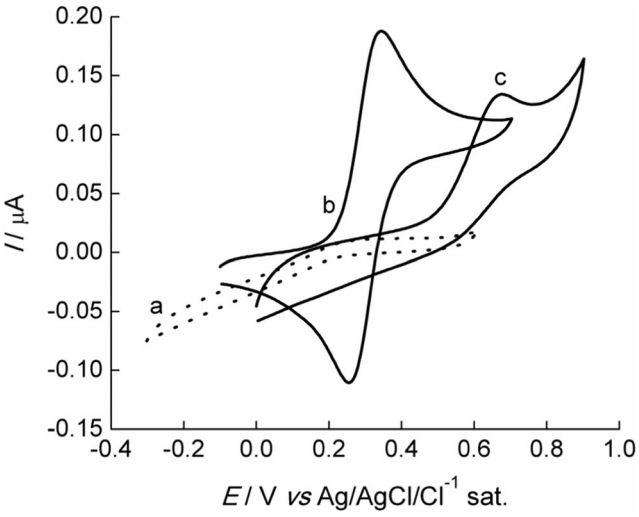

Fig. 5 Cyclic voltammogram of 1×10^{-3} mol L^{-1} $K_3[Fe(CN)_6]$ (curve a), 1×10^{-4} mol L^{-1} $FcCO_2H$ (curve b), 6×10^{-5} mol L^{-1} thymol at a SAM electrode of HS-β-CD (curve c) in 0.2 mol L^{-1} Na_2SO_4. Scan rates = 10 mVs^{-1}

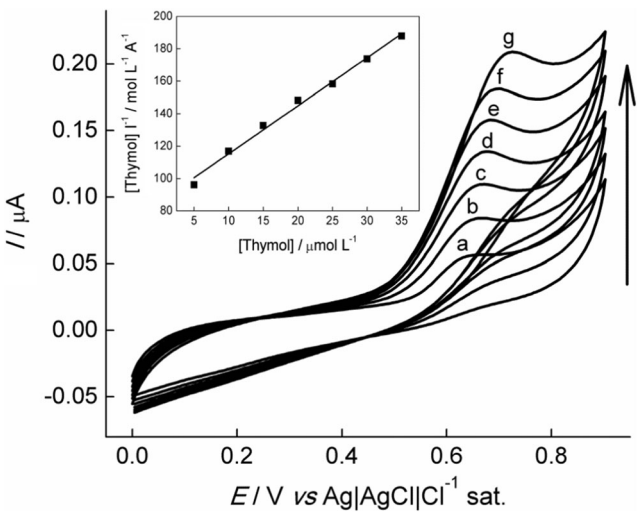

Fig. 6 Cyclic voltammograms recorded in 0.2 mol L^{-1} Na_2SO_4 solution for the detection of various concentrations of thymol: (from 5 to 35 µmol L^{-1}) using GCE. Inset graph: Plot of peak current versus different concentrations of thymol for GCE

apparent formation constant (K_F) of the thymol- β-CD complex, experimental data were analyzed using the Benesi-Hildebrand method [40]. According to this approach, the dissociation constant of the complex can be calculated by Eq. 3, followed by the fit to the Benesi-Hildebrand equation in wavelength from $\lambda = 274$ nm at a contact time of 1 h (Fig. 7).

$$\frac{[C]_0[S]_0}{\Delta A} = \frac{K_D}{\Delta\varepsilon} + \frac{[C]_0}{\Delta\varepsilon} \quad (3)$$

where $[C]_0$ and $[S]_0$ are the initial cyclodextrin and thymol concentrations, respectively. K_D is the dissociation constant and $K_D = 1/K_F$; ΔA is the absorbance change and $\Delta\varepsilon$ is the molar absorption coefficient change. Plotting the values of $[C]_0[S]_0/\Delta A$ versus $[C]_0$ led to a straight line. The slope is $1/\Delta\varepsilon$.

Figure 7 displays the fit to the Benesi-Hildebrand equation in wavelength from $\lambda = 274$ nm at a contact time of 1 h. The formation equilibrium of Thymol-β-CD complex can be written as follows:

$$Thymol + \beta CD \rightleftarrows Thymol{-}\beta CD \quad (4)$$

The stability of the complex can be described regarding this formation K_F or dissociation ($K_D = 1/K_F$) constants:

$$K_F = \frac{[Thymol{-}\beta CDcomplex]}{[Thymol][\beta CD]} \quad (5)$$

From these curve, the dissociation and formation constants were obtained, as 2.80×10^4 L mol^{-1}, which is similar to the value obtained by electrochemical measurements.

Tao and coworkers [23] studied the synthesis and characterization of β-CD inclusion complexes of thymol and found a significant value ($p < 0.05$) of entrapment efficiencies for thymol and β-CD (stoichiometry 1:1). Differential scanning calorimetry (DSC) and phase solubility tests confirmed inclusion complexes formation.

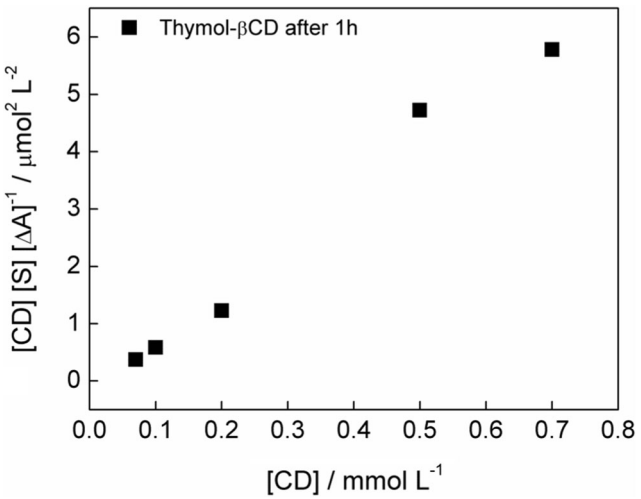

Fig. 7 Benesi-Hildebrand graph: plot of the values of [CD] [S]/ΔA versus [CD]. [S] = [Thymol] = 1.0×10^{-4} mol L^{-1}; [CD] = 5.0×10^{-5} to 7.0×10^{-4} mol L^{-1}. Contact time 1 h

Calibration curve and limit of detection of thymol using SAM electrode

The analytical performance of the voltammetry method developed for thymol determination was evaluated using (SAM)-modified GE of HS-β-CD, at different concentrations of thymol. To improve the selectivity and limit of detection for thymol, different strategies used to modify the electrode surface was employed. These include modification by SAM,

From Fig. 8, the DPV recorded for increasing amounts of thymol using the optimized parameters showed that the peak current increases with the analyte concentration over the range used. The oxidative peak current of thymol was selected as the analytical signal. The result showed that the oxidative peak current was proportional to the concentration of thymol in the range from 1 to 50 μmol L^{-1}. The detection limit (DL) of SAM-modified GE was 1.43×10^{-5} mol L^{-1}, meanwhile the quantification limit (QL) was 4.76×10^{-5} mol L^{-1}. These values showed that SAM Au/cyclodextrin modified electrodes are a top working electrode and can be applied for analysis for thymol determination.

Scanning electrochemical microscopy of thymol-β-CD complex

Scanning electrochemical microscopy (SECM) has been extensively used in recent years, since it enables the point of an ultra-micro-electrode to be used to obtain images of different

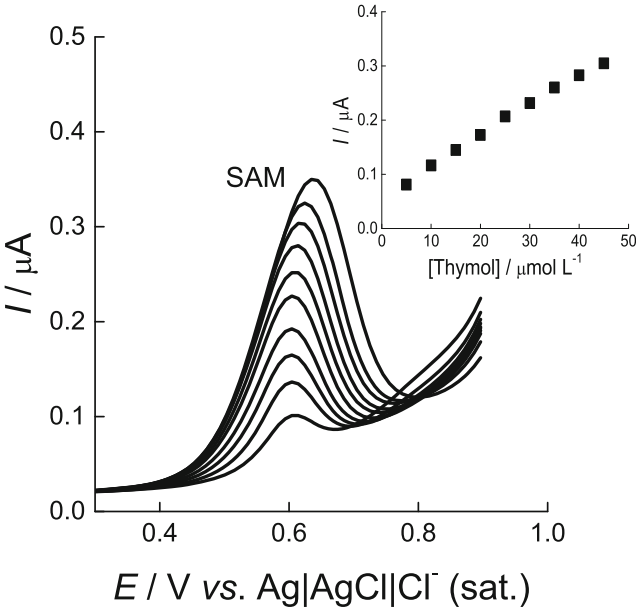

Fig. 8 Differential pulse voltammograms recorded in 0.2 mol L^{-1} Na_2SO_4 solution for the detection of various concentrations of thymol: (1 to 50 μmol L^{-1}), using SAM-modified GE of HS-β-CD. Inset graph: Plot of peak current versus different concentrations of thymol for two kind of modified electrodes. Pulse amplitude = 50 mV, pulse time = 70 ms, $v = 0.01$ mVs^{-1}

surfaces of substrate immersed in an electrolytic solution, with micrometric resolution. In the present study, SECM was also used to observe the electrochemical interaction between a layer of dsDNA, thymol, and thymol-β-CD complex, making it possible to obtain images of the surface of this biosensor before and after interaction with thymol.

As mentioned in the experiment, ferrocene methanol was used as redox mediator with feedback mode. Figure 9 shows the surface of a glassy carbon electrode without modification (Fig. 9a) and modified with dsDNA (Fig. 9b). It can be seen that the glassy carbon (GC) and dsDNA/GC exhibit homogeneous electrochemical activity, as the GC shows itself to be a common substrate with conductive behavior, with current values 1.25 higher than in the stationary state [31]. The normalized current decreased from 1.25 to 1.0 in presence of dsDNA on the surface of GC. This behavior is compatible with a negative feedback between the point of the ultra-micro-electrode and the substrate, indicating that dsDNA partially blocks the electrochemical response of the ferrocene methanol (FcOH) redox mediator.

When thymol is present in dsDNA/GC (Fig. 9c), the images show that the normalized current increases are achieving currents of the redox mediator similar to those observed on bare glassy carbon. This behavior can be explained by the disorganization of the dsDNA layer by the interaction with thymol causing the desorption of DNA. On the other hand, when dsDNA/GC is evaluated in the presence of the thymol-*β-CD* inclusion complex (Fig. 9d), the conductivity was similar to that of the dsDNA film. This result is indicative of significantly lower interaction of Thymol with the DNA macromolecule, because thymol is encapsulated into a β-CD cavity. These results are in agreement with the study of the interaction between thymol and dsDNA, carried out using an EQCM, DPV, and AFM.

The use of the inclusion complex of thymol:β-CD to reduce thymol toxicity by lowering its availability to interact with DNA is proposed here for the first time. As demonstrated above according to our EQCM, AFM, and DPV results, the ability of thymol to bind and alter specific properties of DNA justifies the necessity of the characterization of inclusion complex containing thymol and β-CD.

The characterization of inclusion complexes containing thymol and β-CD by measuring the interaction between these two components and the ability of thymol to bind DNA in its free and β-cyclodextrin complexed form were evaluated by highly specialized techniques. The use of β-CD to encapsulate hydrophobic substances has garnered increased interest over the past decade given its potential role in improving drug delivery regimens. The encapsulation approach is particularly useful when controlled target release is desired, and a compound is insoluble, unstable, or DNA toxic. Thymol exhibits several of these characteristic properties and represents a potential candidate for complexation with cyclodextrin as a promising delivery option [41].

EQCM, AFM, and DPV were employed to determinate the DNA-binding properties of thymol that are reflective of genotoxicity. The combined use of voltammetry and UV-vis

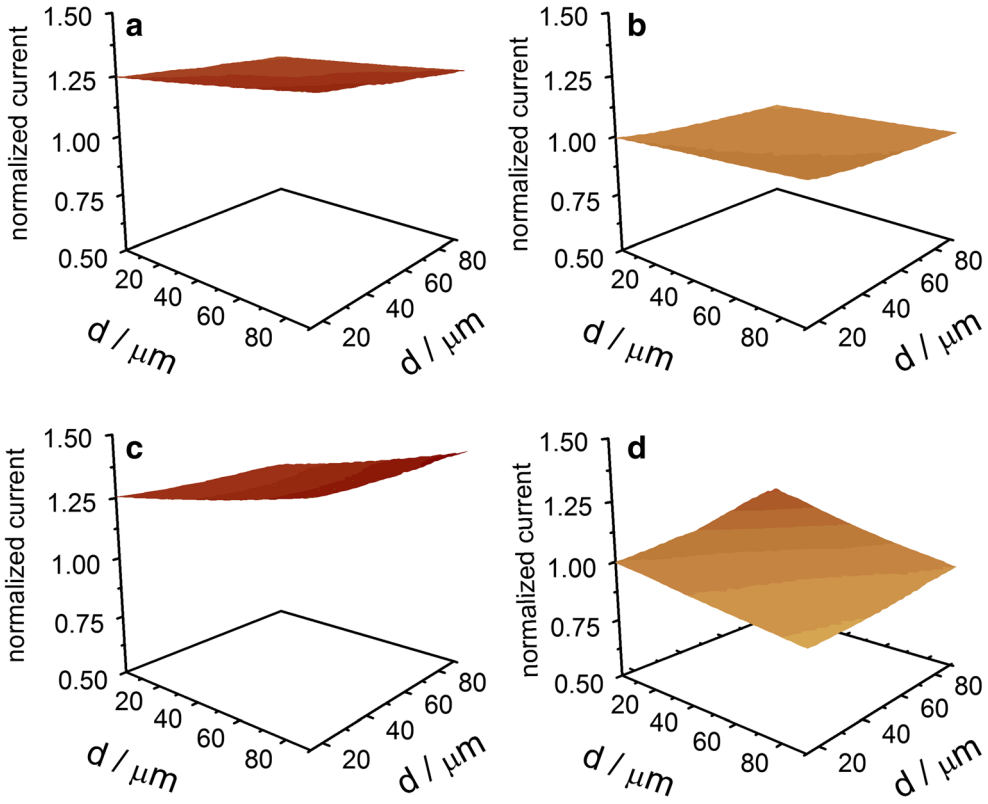

Fig. 9 SECM surface-plot images of bare glassy carbon electrode (**a**), dsDNA/GC electrode (**b**) dsDNA/GC electrode in presence of thymol solution (**c**) and dsDNA/GC electrode in presence of thymol: β-CD inclusion complex in solution (**d**). The images were made with a carbon fiber tip positioned at about 10 μm of distance. 0.01 mol L^{-1} ferrocene methanol in 0.2 mol L^{-1} phosphate buffer (pH 7.4) was used as a redox mediator

spectrophotometry facilitates characterization of thymol-β-CD interactions. In the same way, the SECM was applied to investigate the DNA-binding properties of thymol and thymol-β-CD inclusion complex.

Conclusions

Herein is the first study using several robust techniques to corroborated DNA interaction and damage of thymol in the absence and presence of β-CD. First, we studied thymol in and its interactions with DNA, to shed further light on the genotoxicity, bioavailability, and reactivity of this biologically active molecule. Using an electrochemical quartz crystal microbalance (EQCM), it was possible to follow the formation of self-organized monolayers of aminoethane thiol linked to dsDNA, determine the quantity of molecule deposited on each layer, and also to observe and confirm the interaction between thymol with dsDNA. The genotoxic potential of thymol was evaluated using the atomic force microscopy (AFM) and corroborated by DPV. The AFM results exhibit a high genotoxic potential on dsDNA despite the low level of thymol inducing noticeable conformational changes in dsDNA and damage. DPV shows DNA damage recorded in guanine and adenine bases.

The study of the thymol: β-CD complex on DNA and their possible resulting genotoxicity effects were achieved by scanning electrochemical microscopy (SECM), electrochemical, and UV-vis experiments. SECM results showed that the thymol: β-CD inclusion complex formed decrease interaction of thymol with the DNA. That leads us to conclude that when encapsulated in β-CD, thymol is partially unavailable to interact with DNA, which probably reduces its toxicity. Nevertheless, it is important to ensure that encapsulation does not remove chemical and biological properties from thymol. Fortunately, previous work has shown that this encapsulation process in many cases improves the properties of thymol. Electrochemical analysis and UV-vis spectrophotometry prove that thymol forms inclusion complex with β-CD. The apparent formation constant (K_F) from UV-vis using the Benesi-Hildebrand equation in the aqueous solution of thymol-β-CD inclusion complex was 2.8×10^4 L mol^{-1}, at a molar ratio 1:1. Also electroanalytical studies showed that SAM Au/cyclodextrin-modified electrodes are a top working electrode and can be used for analysis for thymol determination.

Acknowledgements The authors are grateful to Brazilian agencies CNPq, CAPES, FAPEAL, and Organization of American States (OAS) for financial support.

References

1. Marchese A, Orhan IE, Daglia M et al (2016) Antibacterial and antifungal activities of thymol: a brief review of the literature. Food Chem 210:402–414
2. Jukić M, Miloš M (2005) Catalytic oxidation and antioxidant properties of thyme essential oils (*Thymus vulgarae L.*) Croat Chem Acta 78:105–110
3. Monteiro MVB, de Melo Leite AKR, Bertini LM et al (2007) Topical anti-inflammatory, gastroprotective and antioxidant effects of the essential oil of *Lippia sidoides* Cham. leaves. J Ethnopharmacol 111:378–382
4. Del Nobile MA, Conte A, Incoronato AL, Panza O (2008) Antimicrobial efficacy and release kinetics of thymol from zein films. J Food Eng 89:57–63
5. Du E, Gan L, Li Z et al (2015) In vitro antibacterial activity of thymol and carvacrol and their effects on broiler chickens challenged with *Clostridium perfringens*. J Anim Sci Biotechnol 6:58
6. Özgüven M, Tansi S (1998) Drug yield and essential oil of Thymus vulgaris L. as in influenced by ecological and ontogenetical variation. Turkish J Agric For 22:537–542
7. Bakkali F, Averbeck S, Averbeck D, Idaomar M (2008) Biological effects of essential oils—a review. Food Chem Toxicol 46:446–475
8. Baydar H, Sağdiç O, Özkan G, Karadoğan T (2004) Antibacterial activity and composition of essential oils from Origanum, Thymbra and Satureja species with commercial importance in Turkey. Food Control 15:169–172
9. Vardar-Ünlü G, Candan F, Sókmen A et al (2003) Antimicrobial and antioxidant activity of the essential oil and methanol extracts of *Thymus pectinatus* Fisch. et Mey. Var. pectinatus (Lamiaceae). J Agric Food Chem 51:63–67
10. Da Silveira Novelino AM, Daemon E, Soares GLG (2007) Evaluation of the acaricide effect of thymol, menthol, salicylic acid, and methyl salicylate on Boophilus Microplus (Canestrini 1887) (Acari: Ixodidae) larvae. Parasitol Res 101:809–811
11. Shapiro S, Meier A, Guggenheim B (1994) The antimicrobial activity of essential oils and essential oil components towards oral bacteria. Oral Microbiol Immunol 9:202–208
12. Manou I, Bouillard L, Devleeschouwer MJ, Barel AO (1998) Evaluation of the preservative properties of Thymus vulgaris essential oil in topically applied formulations under a challenge test. J Appl Microbiol 84:368–376
13. Stammati A, Bonsi P, Zucco F et al (1999) Toxicity of selected plant volatiles in microbial and mammalian short-term assays. Food Chem Toxicol 37:813–823
14. Azirak S, Rencuzogullari E (2008) The in vivo genotoxic effects of carvacrol and thymol in rat bone marrow cells. Environ Toxicol. https://doi.org/10.1002/tox.20380
15. Ündeger Ü, Basaran A, Degen GH, Basaran N (2009) Antioxidant activities of major thyme ingredients and lack of (oxidative) DNA damage in V79 Chinese hamster lung fibroblast cells at low levels of carvacrol and thymol. Food Chem Toxicol 47:2037–2043
16. Aydin S, Başaran AA, Başaran N (2005) The effects of thyme volatiles on the induction of DNA damage by the heterocyclic amine IQ and mitomycin C. Mutat Res Genet Toxicol Environ Mutagen 581:43–53
17. Buyukleyla M, Rencuzogullari E (2009) The effects of thymol on sister chromatid exchange, chromosome aberration and micronucleus in human lymphocytes. Ecotoxicol Environ Saf 72:943–947
18. Messner M, Kurkov SV, Jansook P, Loftsson T (2010) Self-assembled cyclodextrin aggregates and nanoparticles. Int J Pharm 387:199–208
19. Brewster ME, Loftsson T (2007) Cyclodextrins as pharmaceutical solubilizers. Adv Drug Deliv Rev 59:645–666

20. Marques HMC (2010) A review on cyclodextrin encapsulation of essential oils and volatiles. Flavour Fragr J 25:313–326
21. Sanguansri P, Augustin MA (2006) Nanoscale materials development—a food industry perspective. Trends Food Sci Technol 17: 547–556
22. Mulinacci N, Melani F, Vincieri FF et al (1996) 1H-NMR NOE and molecular modelling to characterize thymol and carvacrol b-cyclodextrin complexes. Int J Pharm 128:81–88
23. Tao F, Hill LE, Peng Y, Gomes CL (2014) Synthesis and characterization of β-cyclodextrin inclusion complexes of thymol and thyme oil for antimicrobial delivery applications. LWT - Food Sci Technol 59:247–255
24. Polyakov NE, Leshina TV, Konovalova TA et al (2004) Inclusion complexes of carotenoids with cyclodextrins: ^{1}H NMR, EPR, and optical studies. Free Radic Biol Med 36:872–880
25. Moore KE, Flavel BS, Ellis AV, Shapter JG (2011) Comparison of double-to single-walled carbon nanotube electrodes by electrochemistry. Carbon N Y 49:2639–2647
26. Loaiza ÓA, Campuzano S, López-Berlanga M et al (2005) Development of a DNA sensor based on alkanethiol self- assembled monolayer-modified electrodes. Sensors 5:344–363
27. Lyubchenko Y, Shlyakhtenko L, Harrington R et al (1993) Atomic force microscopy of long DNA: imaging in air and under water. Proc Natl Acad Sci U S A 90:2137–2140
28. Bustamante C, Vesenka J, Tang CL et al (1992) Circular DNA molecules imaged in air by scanning force microscopy. Biochemistry 31:22–26
29. Allen MJ, Dong XF, O'Neill TE et al (1993) Atomic force microscope measurements of nucleosome cores assembled along defined DNA sequences. Biochemistry 32:8390–8396
30. de Vasconcellos MCMC, De Oliveira Costa C, da Silva Terto EGEG et al (2016) Electrochemical, spectroscopic and pharmacological approaches toward the understanding of biflorin DNA damage effects. J Electroanal Chem 765:168–178
31. Bollo S, Ferreyra NF, Rivas GA (2007) Electrooxidation of DNA at glassy carbon electrodes modified with multiwall carbon nanotubes dispersed in chitosan. Electroanalysis 19:833–840
32. Sadik OA, Aluoch AO, Zhou A (2009) Status of biomolecular recognition using electrochemical techniques. Biosens Bioelectron 24:2749–2765
33. Nowicka AM, Kowalczyk A, Stojek Z, Hepel M (2010) Nanogravimetric and voltammetric DNA-hybridization biosensors for studies of DNA damage by common toxicants and pollutants. Biophys Chem 146:42–53
34. Cerreta A, Vobornik D, Di Santo G et al (2012) FM-AFM constant height imaging and force curves: high resolution study of DNA-tip interactions. J Mol Recognit 25:486–493
35. Pang D, Thierry AR, Dritschilo A (2015) DNA studies using atomic force microscopy: capabilities for measurement of short DNA fragments. Front Mol Biosci 2:1–7
36. Sawant PD, Watson GS, Nicolau D et al (2005) Hierarchy of DNA immobilization and hybridization on poly-L-lysine using an atomic force microscopy study. J Nanosci Nanotechnol 5:951–957
37. Nafisi S, Hajiakhoondi A, Yektadoost A (2004) Thymol and carvacrol binding to DNA: model for drug-DNA interaction. Biopolymers 74:345–351
38. Maeda Y, Fukuda T, Yamamoto H, Kitano H (1997) Regio- and stereoselective complexation by a self-assembled monolayer of thiolated cyclodextrin on a gold electrode. Langmuir 13:4187–4189
39. Damos FS, Luz RCS, Kubota LT (2007) Electrochemical properties of self-assembled monolayer based on mono-(6-deoxy-6-mercapto)-b-cyclodextrin toward controlled molecular recognition. Electrochim Acta 53:1945–1953
40. Hernández-Benito J, González-Mancebo S, Calle E et al (1999) A practical integrated approach to supramolecular chemistry. I. Equilibria in inclusion phenomena. J Chem Educ 76:419
41. Nieddu M, Rassu G, Boatto G, Bosi P, Trevisi P, Giunchedi P, Carta AGE, Nieddu M, Rassu G et al (2014) Improvement of thymol properties by complexation with cyclodextrins: in vitro and in vivo studies. Carbohydr Polym 102:393–399